Published in final edited form as:
Free Radic Biol Med. 2014 August ; 0: 51–59. doi:10.1016/j.freeradbiomed.2014.04.014.

Inducible nitric oxide synthase is key to peroxynitrite-mediated, LPS-induced protein radical formation in murine microglial BV2 cells

Ashutosh Kumar[1,*], **Shih-Heng Chen**[2], **Maria B. Kadiiska**[1], **Jau-Shyong Hong**[2], **Jacek Zielonka**[3], **Balaraman Kalyanaraman**[3], and **Ronald P. Mason**[1]

[1]Free Radical Metabolism Group, Laboratory of Toxicology & Pharmacology, National Institute of Environmental Health Sciences, National Institutes of Health, Research Triangle Park, North Carolina, 27709, USA

[2]Neuropharmacology Group, Laboratory of Toxicology & Pharmacology, National Institute of Environmental Health Sciences, National Institutes of Health, Research Triangle Park, North Carolina, 27709, USA

[3]Department of Biophysics and Free Radical Research Center, Medical College of Wisconsin, Milwaukee, WI 53226, USA

Abstract

Microglia are the resident immune cells in the brain. Microglial activation is characteristic of several inflammatory and neurodegenerative diseases including Alzheimer's disease, multiple sclerosis, and Parkinson's disease. Though LPS-induced microglial activation in models of Parkinson's disease (PD) is well documented, the free radical-mediated protein radical formation and its underlying mechanism during LPS-induced microglial activation is not known. Here we have used immuno-spin trapping and RNA interference to investigate the role of inducible nitric oxide synthase (iNOS) in peroxynitrite-mediated protein radical formation in murine microglial BV2 cells treated with LPS.

Treatment of BV2 cells with LPS resulted in morphological changes, induction of iNOS and increased protein radical formation. Pretreatments with FeTPPS (a peroxynitrite decomposition catalyst), L-NAME (total NOS inhibitor), 1400W (iNOS inhibitor) and apocynin significantly attenuated LPS-induced protein radical formation and tyrosine nitration. Results obtained with coumarin-7-boronic acid, a highly specific probe for peroxynitrite detection, correlated with LPS-induced tyrosine nitration, which demonstrated involvement of peroxynitrite in protein radical formation. A similar degree of protection conferred by 1400W and L-NAME led us to conclude that only iNOS, and no other forms of NOS, are involved in LPS-induced peroxynitrite formation.

[*]**Author for correspondence:** Dr. Ashutosh Kumar, Free Radical Metabolism Group, Laboratory of Toxicology and Pharmacology, 111 T.W. Alexander Dr., Research Triangle Park, North Carolina 27709, USA. kumara10@niehs.nih.gov Tel: (919)-541-3866.

Conflict of interest: The authors declare no conflict of interest.

Subsequently, siRNA for iNOS, the iNOS-specific inhibitor 1400W, the NF-kB inhibitor PDTC and the P38 MAPK inhibitor SB202190 were used to inhibit iNOS directly or indirectly. Inhibition of iNOS precisely correlated with decreased protein radical formation in LPS-treated BV2 cells. The time course of protein radical formation also matched the time course of iNOS expression. Taken together, these results prove the role of iNOS in peroxynitrite-mediated protein radical formation in LPS-treated microglial BV2 cells.

Keywords

LPS; Nitrone adducts; Protein radical; Peroxynitrite; Microglia; Inducible nitric; oxide synthase; Parkinson's disease

Introduction

Parkinson's disease is the second most common neurodegenerative disease of the aging brain and manifests itself mostly as a sporadic condition [1, 2]. Microglia-mediated neuroinflammation is considered to be a priming event in onset and progression of Parkinson's disease [3–5]. The transformation of microglia into potentially toxic activated microglia takes place in response to even subtle disturbances in the brain microenvironment [4]. The activation of microglia takes place in almost every type of neurological disorder and is often associated with the release of proinflammatory cytokines and an increased production of superoxide ($O_2^{\bullet -}$) and nitric oxide ($NO^{\bullet}$). $NO^{\bullet}$ and $O_2^{\bullet -}$ react to form the neurotoxic peroxynitrite ($ONOO^-$), which has been implicated in Parkinson's disease, in part because the level of nitrotyrosine, a product of the reaction of peroxynitrite with tyrosine, increases in Parkinson's disease [6–8].

Lipopolysaccharide (LPS), an endotoxin released from the outer membranes of Gram-negative bacteria, activates microglial cells, and the over-secreted products, in turn, are cytotoxic to neurons. Activation of NADPH oxidase by LPS triggers excessive $O_2^{\bullet -}$ generation, which eventually exacerbates the inflammatory response [9, 10]. LPS also induces selective expression of iNOS, which contributes to $NO^{\bullet}$ production and subsequent formation of peroxynitrite due to concurrent production of $O_2^{\bullet -}$ from NADPH oxidase during the microglial activation process [11, 12].

Though LPS-induced microglial activation is well known, the underlying mechanism of peroxynitrite-mediated protein radical formation within microglia is not known. Understanding the mechanism of protein radical formation during microglial activation is important for defining targets that might be useful in minimizing proteotoxic stress and inflammation, which is crucial in the onset and progression of several neurodegenerative diseases. Possible biochemical consequences of protein radical formation may involve changes in activity, triggering immunogenic responses, alteration in protein assembly and formation of proteasome-resistant aggregates [13]. Nitration of a single tyrosine residue on Hsp90 is documented to convert it from a prosurvival protein into a potent mediator of neuronal death [14].

The formation of free radicals resulting from microglial activation, which may have dire consequences for both microglia and neurons, has not received the attention it deserves, mostly due to the limitations of detecting free radicals in biological systems. To overcome these limitations, we used the highly sensitive immuno-spin-trapping technique [15] to investigate protein radical formation during LPS-induced microglial activation. Though it used to be problematic to establish an unambiguous link between peroxynitrite and protein radical formation in biological systems due to limitations of specific detection of peroxynitrite, recent advancements in peroxynitrite detection using fluorogenic boronate probes has made this possible [16, 17]. Specifically, coumarin-7-boronic acid reacts stoichiometrically and rapidly with peroxynitrite to form hydroxycoumarin, which exhibits blue fluorescence and facilitates specific detection of peroxynitrite [16, 17]. Therefore, we used coumarin-7-boronic acid based peroxynitrite detection to demonstrate its involvement in LPS-induced protein radical formation.

Here we report for the first time that LPS induces protein radical formation in murine microglial BV2 cells, which is peroxynitrite-mediated, and that iNOS plays a crucial role. Furthermore, we report an interaction between iNOS signaling and protein radical formation in microglial BV2 cells. The information gathered in this study will provide new insights on involvement of protein radicals in microglia-mediated neurodegenerative disorders.

Materials and Methods

Materials

The murine microglial BV2 cell line was obtained from the neuropharmacology lab, NIEHS (Research Triangle Park, NC). Coumarin-7-boronic acid (CBA) was synthesized as described earlier [18]. LPS (Escherichia coli 0111:B4) was purchased from Calbiochem (La Jolla, CA) and was reconstituted in ultrapure water and kept at 4°C. Apocynin, L-ω-nitroarginine methyl ester (L-NAME), *N*-3-(aminomethyl)benzylacetamide.2HCl (1400W), paraformaldehyde, phorbolmyristate acetate (PMA), pyrrolidine dithiocarbamate (PDTC), 5,10,15,20-tetrakis(4-sulfonatophenyl) porphyrinato iron (III) chloride (FeTPPS), SB 202190, sodium nitrite, and TNFα were from Sigma (St. Louis, MO). DMPO was obtained from Dojindo Laboratories (Rockville, MD) and used without further purification. Chicken polyclonal anti-DMPO antibodies were developed in our laboratory and used in the immuno-spin-trapping studies. Rabbit polyclonal anti-iNOS antibody and siRNA against iNOS were from Santa Cruz Biotechnology (Dallas, TX). Rabbit polyclonal anti-3-nitro tyrosine was from Abcam (Cambridge, MA). Lipofectamine RNAiMAX reagent and transfection media were from Invitrogen (Grand Island, NY).

Cell culture and treatments with LPS, DMPO and various inhibitors

Murine microglial BV2 cells were cultured in high glucose Dulbecco's modified Eagle's medium, supplemented with 10 % heat-inactivated fetal bovine serum, 50 U/ml penicillin, and 50 μg/ml of streptomycin. Cells were maintained in a humidified atmosphere of 5% CO_2 at 37°C and cultured in T-75 Falcon tissue culture flasks at an initial density of 1×10^6 cells/flask. The culture medium was replenished on day 2 and changed on day 5. BV2 cells were treated with FeTPPS (10 μM), L-NAME (100 μM), apocynin (1 mM) or 1400W (10

μM) for 2 hours prior to LPS treatment. Afterwards, cells were treated with LPS (500 ng/ml)-containing medium for another 24 hours, while inhibitors remained in the culture medium. Typically, cells were incubated for 24 hours in complete medium containing 500 ng/ml LPS and 50 mM DMPO.

Measurement of peroxynitrite formation by monitoring oxidation of coumarin-7-boronic acid

BV2 cells were grown in phenol-free DMEM medium as mentioned above. Cells were incubated with LPS (500 ng/ml) for 21 hours and then coumarin-7-boronic acid was added (20 μM); fluorescence intensities were monitored immediately after coumarin-7-boronic acid addition using a Tecan SpectraFluor-Plus plate reader (Research Triangle Park, NC) equipped with the appropriate excitation (320 nm) and emission (430 nm) filters. The instrument was prewarmed and kept at 37°C during measurements, and fluorescence intensity read from the top of each well was recorded every 10 minutes for 180 minutes. In other experiments, cells were incubated with LPS (500 ng/ml) and TNFα (50 ng/ml) for 21 hours, and then co-treated with coumarin-7-boronic acid and PMA (200 ng/ml) in the same medium before monitoring fluorescence.

Confocal microscopy of cells

2×10^5 BV2 cells were incubated overnight at 37°C on glass coverslips, followed by the treatments mentioned above. To localize nitrone adducts after the treatments, the cells were fixed with 4% paraformaldehyde for 15 minutes at room temperature, washed twice for 5 minutes, permeabilized for 5 minutes with 0.5% Triton X-100 in PBS (pH 7.4), and washed twice for 5 minutes. After blocking with 4% fish gelatin in PBS (pH 7.4) overnight at 4°C, the cells were incubated with chicken polyclonal anti-DMPO (diluted 1:2,000) for 2 h, followed by secondary anti-chicken AlexaFluor 488 (diluted 1:1,000) for 1 h. Then coverslips were washed four times and mounted on glass slides using Prolong Gold anti-fade reagent with DAPI. Confocal images were snapped on a Zeiss LSM 510-UV meta microscope (Carl Zeiss Inc, Oberkochen, Germany) using a Plan-NeoFluar 40×/1.3 Oil DIC objective.

Assessment of morphological changes

2×10^5 BV2 cells were incubated overnight at 37°C on glass coverslips, followed by treatment with LPS for 24 hours. Images of these cells were taken directly under an inverted phase contrast microscope at 40× magnification.

Determination of total nitrone adducts in cells

Cell lysates for use in ELISA or Western blotting for the detection of DMPO-protein nitrone adducts were prepared by scraping cells in RIPA buffer (0.05 g of sodium deoxycholate, 100 μl of Triton X-100, and 10 μl of 10% SDS in 10 ml of 0.1M PBS) containing protease inhibitors. After a 30-min incubation of the scraped samples in ice, samples were centrifuged at 20,000 g for 20 min. The soluble fraction (supernatant) was stored at 4°C until use. Nuclear/cytosolic fractionation was also carried out in some samples using a nuclear/cytosolic fractionation kit from BioVision (Mountain View, CA) to determine the cellular

distribution of nitrone adducts. Rabbit polyclonal anti-DMPO antibody was used to detect DMPO-protein-derived nitrone adducts using a standard ELISA in all samples [19].

RNA interference

2.5×10^5 BV2 cells were seeded in 6-well plates in antibiotic-free normal growth medium and incubated for 24 hours to attain 60% confluence. siRNAs for iNOS were used with Lipofectamine RNAiMAX reagent following the manufacturer's instructions (Invitrogen, Grand Island, NY) for transfection. Forty-eight hours after transfection, cells were incubated with LPS (500 ng/ml) for 24 hours and then harvested for total protein extraction. Western blot using an iNOS antibody was performed to assess the extent of inhibition.

Statistical analysis

One-way analysis of variance (ANOVA) was used for statistical analysis. The Newman–Keuls post-test was used for multiple comparisons. The results are expressed as mean ± SEM. The differences were considered statistically significant when p values were less than 0.05.

Results

LPS induces morphological changes and protein radical formation in BV2 cells

BV2 cells treated with increasing concentrations of LPS for 24 hours underwent dramatic morphological changes characterized by vacuolization (at 1000 ng/ml of LPS) and hypertrophy, especially at higher concentrations of LPS (Figure 1). Even low concentrations of LPS induce signaling cascade and microglial activation [20]; however, to ensure a detectable protein radical formation, we used 500 ng/ml of LPS to activate BV2 cells; this concentration of LPS induced the maximum level of nitrite and had no significant cytotoxicity to BV2 cells [10].

Immuno-spin trapping experiments with LPS-treated BV2 cells showed intense anti-DMPO staining (Figure 2A), which gives strong evidence of protein radical formation. Confocal images showed cytosolic staining in LPS-treated BV2 cells, which was attenuated significantly by pretreatment with a peroxynitrite decomposition catalyst (FeTPPS), a total NOS inhibitor (L-NAME), an iNOS inhibitor (1400W) and apocynin (Figure 2A). In order to specifically quantify the DMPO nitrone adducts in different cell-compartments, we separated the cytosolic and the nuclear fractions and analyzed them by ELISA (Figure 2B). The cytosolic fraction had much higher levels of DMPO nitrone adducts, which indicated that the anti-DMPO signal was mostly from cytosolic proteins and not or minimally from DNA. We quantified protein-derived radicals with anti-DMPO ELISA (Figure 2C), which showed concurrence with the confocal images (Figure 2A). All pretreatments were significantly effective in mitigating LPS-induced protein radical formation. A similar degree of inhibition was conferred by the relatively specific iNOS inhibitor (1400W) and broad-spectrum NOS inhibitor (L-NAME) (Figure 2C), leading us to conclude that only iNOS and no other forms of NOS (eNOS or nNOS) are involved in LPS-induced protein radical formation.

LPS-induced protein radical formation in BV2 cells is peroxynitrite-mediated

LPS-induced microglial activation is often associated with NADPH oxidase activation and iNOS induction [11, 12]. Therefore, we looked for peroxynitrite generation as a possible mechanism for protein radical formation in BV2 cells. To investigate the role of peroxynitrite in LPS-induced protein radical formation, we analyzed BV2 cells exposed to LPS in the presence and absence of various inhibitors using anti-3-nitro tyrosine staining and ELISA. Tyrosine nitration as an indirect measure of peroxynitrite generation was significantly attenuated by pretreatments with a peroxynitrite decomposition catalyst (FeTPPS), a total NOS inhibitor (L-NAME), an iNOS inhibitor (1400W) and apocynin (Figure 3A, B). The similar extent of inhibition by the relatively specific iNOS inhibitor (1400W) and the total NOS inhibitor (L-NAME) further indicated that iNOS is the key to peroxynitrite generation. The obvious tyrosine nitration and its concurrence with protein radical formation prompted us to monitor the real time generation of peroxynitrite in a more specific manner.

Real time monitoring of peroxynitrite in LPS-induced BV2 cells

To confirm the involvement of peroxynitrite in LPS-induced BV2 cells, we used coumarin-7-boronic acid, a boronate based fluorogenic probe that selectively reacts with peroxynitrite [17]. It is noteworthy that the chemistry and mechanisms of reaction of H_2O_2 and peroxynitrite with most boronates are very similar [21]; therefore, we used a targeted boronic acid-based fluorophore coumarin-7-boronic acid, which is specific for detection of peroxynitrite [17]. Activation of BV2 cells with only LPS led to mild but significant oxidation of coumarin-7-boronic acid as evidenced by increased fluorescence with time (Figure 4A). The increase in fluorescence as a measure of peroxynitrite generation was more pronounced when cells were activated by LPS, TNF α, and phorbolmyristate acetate (PMA) than in cells stimulated with LPS alone (Figure 4 B). Addition of superoxide dismutase (SOD) to activated BV2 cells significantly reduced coumarin-7-boronic acid-derived fluorescence. SOD-mediated reduction in coumarin-7-boronic acid-derived fluorescence indicated impaired peroxynitrite generation due to effective dismutation of superoxide and, therefore, indicated the specificity of coumarin-7-boronic acid for peroxynitrite. Furthermore, because SOD cannot enter cells, much of the detected peroxynitrite formation is apparently extracellular. Simultaneously, the absence of any significant effect by catalase, which catalyzes decomposition of H_2O_2, further indicated specificity of this probe towards peroxynitrite. Thus, under conditions generating both H_2O_2 and peroxynitrite, CBA appeared to react primarily with peroxynitrite. Inhibition of coumarin-7-boronic acid-derived fluorescence by 1400W further confirmed the role of iNOS in LPS-induced peroxynitrite generation.

iNOS expression is crucial to peroxynitrite-mediated protein radical formation in LPS-induced BV2 cells

In order to investigate the correlation between iNOS-mediated peroxynitrite generation and protein radical formation in LPS-induced BV2 cells, we performed a time-course study, which showed a concurrence between iNOS expression and protein radical formation, with both peaking 18–24 hours after LPS exposure (Figure 5). Taken together with previous

results, the concurrence of iNOS expression and protein radical formation indicated causality between them.

To further confirm the role of iNOS in peroxynitrite-mediated protein radical formation, iNOS in BV2 cells was silenced using different siRNAs and inhibited using several signaling inhibitors such as the NF-Kβ inhibitor PDTC or P38 MAP kinase inhibitor SB202190. The siRNA-mediated iNOS gene-silencing and the iNOS signaling inhibitors significantly mitigated iNOS levels in LPS-induced BV2 cells (Figure 6A, B). Anti-DMPO ELISA of LPS-treated BV2 cells showed significant attenuation in protein radical formation when iNOS was silenced or inhibited (Figure 6C). Results from the time course and iNOS inhibition experiments consistently indicated a direct link between iNOS expression and protein radical formation. Taken together, these results confirmed the significant role of iNOS in peroxynitrite-mediated protein radical formation.

Discussion

This is the first report that demonstrates the role of iNOS in peroxynitrite-mediated protein radical formation during LPS-induced microglial activation. Reaction and decay of protein radicals in the cellular milieu is a complex process that depends on the cellular microenvironment [22, 23]. For instance, these radicals may react with molecular oxygen to form peroxyl radicals, which eventually decompose to produce oxidation end products [22]. Protein radicals mostly decay to form oxidized and aggregated proteins [24]. Although various models of Parkinson's disease show α-synuclein aggregates forming in the mid brain, the role that protein free radicals play in their formation *in vivo* is unknown, as is the more general question of the role of protein radicals in the onset and progression of Parkinson's disease [25–27]. The detection of protein radicals in microglia can be used to achieve further insights to explore the possible implications of protein radicals in neurodegenerative diseases.

DMPO, a nitrone spin trap which is permeable to the plasma membrane, binds to radicals on macromolecules and enables their detection by immuno-spin trapping [15, 28]. Protein radicals can result from one-electron oxidation of proteins by several reactive moieties such as superoxide and various other free radicals, redox active metals, peroxidases and peroxynitrite-derived radicals [28]. In this study, initial experiments indicated the involvement of NADPH oxidase and iNOS in peroxynitrite-mediated protein radical formation (Figure 2 A–C).

Based on the extent of inhibition by apocynin, NADPH oxidase appeared as the largest single source of superoxide generation leading to peroxynitrite formation in BV2 cells. In addition to NADPH oxidase [29–31] there are other sources, such as mitochondria [32], uncoupling of iNOS [33] and the endoplasmic reticulum [34] which may contribute to superoxide generation. Instead of focusing on these other superoxide sources, we focused primarily on $NO^{\bullet}$-generating nitric oxide synthase isoforms, which contribute to peroxynitrite generation. Eventually, with anti-DMPO staining experiments, it appeared that only iNOS, and no other isoforms of NOS (eNOS and nNOS), contributes to protein radical formation in LPS-challenged BV2 cells.

Interestingly, DMPO has been shown to form adducts in high yield with protein tyrosyl radicals [35–38], and for that reason DMPO-based detection of protein radicals (Figure 2A) and tyrosine nitration (Figure 3A) in this study showed similar patterns. Although tyrosine nitration as an indirect marker of peroxynitrite formation has been documented in various models of neurodegenerative disorders [6, 39, 40], the exclusive role of peroxynitrite in tyrosine nitration has been questioned by several investigators [41, 42]. $^{\bullet}NO_2$ formed through peroxynitrite-independent processes such as myeloperoxidase (MPO) and H_2O_2-catalyzed oxidation of nitrite also leads to tyrosine nitration [39, 41]. However, adding exogenous nitrite could not elicit any additional increase in LPS-induced tyrosine nitration (Supplementary Figure 1), which negated involvement of nitrite/peroxidase chemistry as a significant cause of tyrosine nitration in these cells. This was perhaps due to lack of peroxidase activity in BV2 cells [43, 44]. Furthermore, microglia shows certain similarities with macrophages in which peroxynitrite mediated tyrosine nitration is well documented [45, 46]. Based on these similarities and lack of peroxidase activity in these cells we tried more specific boronate probes to specifically detect the involvement of peroxynitrite in tyrosine nitration and protein radical formation.

Thus, boronate probes, which form measurable products by reacting directly and rapidly with peroxynitrite rather than relying on radical intermediates like $^{\bullet}NO_2$, are a significant advance. Coumarin-7-boronic acid, a boronate probe which specifically reacts with peroxynitrite to give a fluorescent product provides more specific evidence of peroxynitrite generation [17]. It has been repeatedly shown that specific boronates react directly and stoichiometrically with peroxynitrite a million times faster than with H_2O_2 and nearly two hundred times faster than with HOCl and thereby are highly specific even in the cellular systems, which may produce a higher flux of H_2O_2 under proinflammatory conditions [17, 18, 47].

The concurrent formation of superoxide anion radicals and nitric oxide leads to peroxynitrite generation; therefore a relatively strong coumarin-7-boronic acid-derived fluorescence was seen when cells were activated by LPS, TNFα and PMA (Figure 4B). However, a weaker peroxynitrite signal from cells activated by LPS alone appears to be due to a lower flux of $NO^{\bullet}$ from iNOS induction and/or superoxide anion radical [5, 48]. The significant inhibition of coumarin-7-boronic acid-derived fluorescence by SOD, which cannot diffuse through the cell membrane, indicates that peroxynitrite generation is mostly extracellular. Being freely diffusible, $NO^{\bullet}$ produced within microglia diffuses out and reacts with superoxide produced at the surface of the cell membrane by NADPH oxidase. However, due to the detection of a small fraction of SOD-insensitive peroxynitrite, partial intracellular generation may also occur.

The analysis of data from the time course of iNOS induction and protein radical formation indicates a link between iNOS and protein radical formation (Figure 5). Though superoxide generation begins much before iNOS induction, the maximal superoxide generation in microglia is reported to take place 15 hours after LPS treatment [11]. Concurrent higher levels of iNOS in activated microglia led to a higher flux of peroxynitrite, formation of protein radicals, and 3-nitrotyrosine. Furthermore, iNOS inhibition by siRNA or pharmacological inhibitors decreased protein radical formation. The neuroprotection by

gene- silencing of iNOS in various models of Parkinson's disease as shown by several investigators [2, 49] is possibly due to the role of iNOS in peroxynitrite-mediated protein radical formation. Under pathological conditions nitric oxide production results from transcriptional activation of iNOS, which is barely present in the healthy brain [49]. Once induced, iNOS produces sustained high levels of NO, which leads to toxicity via peroxynitrite generation [50].

In conclusion, the present study demonstrates through several lines of evidence that iNOS is key to peroxynitrite-mediated protein radical formation, which might have consequences in several neurodegenerative diseases including Parkinson's disease.

Supplementary Material

Refer to Web version on PubMed Central for supplementary material.

Acknowledgments

The authors gratefully acknowledge Dr. Ann Motten, Jean Corbett, and Mary Mason for their valuable help in the preparation of the manuscript. We are very thankful to Dr. Douglas Ganini and Dr. Thomas van't Erve for reviewing the manuscript.

Grant Support: This work has been supported by the Intramural Research Program of the National Institutes of Health and the National Institute of Environmental Health Sciences.

Abbreviations

The abbreviations used are:

DMPO	5,5-dimethyl-1-pyrroline *N*-oxide
iNOS	inducible nitric oxide synthase
$O_2^{\bullet -}$	superoxide
$NO^{\bullet}$	nitric oxide
$ONOO^-$	peroxynitrite

References

1. Bezard E, Przedborski S. A tale on animal models of Parkinson's disease. Mov. Disord. 2011; 26:993–1002. [PubMed: 21626544]
2. Li M, Dai FR, Du XP, Yang QD, Chen Y. Neuroprotection by silencing iNOS expression in a 6-OHDA model of Parkinson's disease. J. Mol. Neurosci. 2012; 48:225–233. [PubMed: 22638860]
3. Purisai MG, McCormack AL, Cumine S, Li J, Isla MZ, Di Monte DA. Microglial activation as a priming event leading to paraquat-induced dopaminergic cell degeneration. Neurobiol. Dis. 2007; 25:392–400. [PubMed: 17166727]
4. Kreutzberg GW. Microglia: a sensor for pathological events in the CNS. Trends Neurosci. 1996; 19:312–318. [PubMed: 8843599]
5. Qin L, Liu Y, Hong JS, Crews FT. NADPH oxidase and aging drive microglial activation, oxidative stress, and dopaminergic neurodegeneration following systemic LPS administration. Glia. 2013; 61:855–868. [PubMed: 23536230]

6. Xie Z, Wei M, Morgan TE, Fabrizio P, Han D, Finch CE, Longo VD. Peroxynitrite mediates neurotoxicity of amyloid beta-peptide1-42- and lipopolysaccharide-activated microglia. J. Neurosci. 2002; 22:3484–3492. [PubMed: 11978825]
7. Prigione A, Piazza F, Brighina L, Begni B, Galbussera A, Difrancesco JC, Andreoni S, Piolti R, Ferrarese C. Alpha-synuclein nitration and autophagy response are induced in peripheral blood cells from patients with Parkinson disease. Neurosci. Lett. 2010; 477:6–10. [PubMed: 20399833]
8. Ara J, Przedborski S, Naini AB, Jackson-Lewis V, Trifiletti RR, Horwitz J, Ischiropoulos H. Inactivation of tyrosine hydroxylase by nitration following exposure to peroxynitrite and 1-methyl-4-phenyl-1,2,3,6-tetrahydropyridine (MPTP). Proc. Natl. Acad. Sci. U.S.A. 1998; 95:7659–7663. [PubMed: 9636206]
9. Han JE, Choi JW. Control of JNK for an activation of NADPH oxidase in LPS-stimulated BV2 microglia. Arch. Pharm. Res. 2012; 35:709–715. [PubMed: 22553064]
10. Chang RC, Rota C, Glover RE, Mason RP, Hong JS. A novel effect of an opioid receptor antagonist, naloxone, on the production of reactive oxygen species by microglia: a study by electron paramagnetic resonance spectroscopy. Brain Res. 2000; 854:224–229. [PubMed: 10784126]
11. Kaneko YS, Ota A, Nakashima A, Mori K, Nagatsu I, Nagatsu T. Regulation of oxidative stress in long-lived lipopolysaccharide-activated microglia. Clin. Exp. Pharmacol. Physiol. 2012; 39:599–607. [PubMed: 22519637]
12. Sung YH, Shin MS, Ko IG, Kim SE, Kim CJ, Ahn HJ, Yoon HS, Lee BJ. Ulinastatin suppresses lipopolysaccharide-induced prostaglandin E2 synthesis and nitric oxide production through the downregulation of nuclear factorkappaB in BV2 mouse microglial cells. Int. J. Mol. Med. 2013; 31:1030–1036. [PubMed: 23546639]
13. Radi R. Protein tyrosine nitration: biochemical mechanisms and structural basis of functional effects. Acc. Chem. Res. 2013; 46:550–559. [PubMed: 23157446]
14. Franco MC, Ye Y, Refakis CA, Feldman JL, Stokes AL, Basso M, Melero Fernandez de Mera RM, Sparrow NA, Calingasan NY, Kiaei M, Rhoads TW, Ma TC, Grumet M, Barnes S, Beal MF, Beckman JS, Mehl R, Estevez AG. Nitration of Hsp90 induces cell death. Proc. Natl. Acad. Sci. U.S.A. 2013; 110:E1102–E1111. [PubMed: 23487751]
15. Mason RP. Using anti-5,5-dimethyl-1-pyrroline N-oxide (anti-DMPO) to detect protein radicals in time and space with immuno-spin trapping. Free Radic. Biol. Med. 2004; 36:1214–1223. [PubMed: 15110386]
16. Zielonka J, Sikora A, Hardy M, Joseph J, Dranka BP, Kalyanaraman B. Boronate probes as diagnostic tools for real time monitoring of peroxynitrite and hydroperoxides. Chem. Res. Toxicol. 2012; 25:1793–1799. [PubMed: 22731669]
17. Zielonka J, Zielonka M, Sikora A, Adamus J, Joseph J, Hardy M, Ouari O, Dranka BP, Kalyanaraman B. Global profiling of reactive oxygen and nitrogen species in biological systems: high-throughput real-time analyses. J. Biol. Chem. 2012; 287:2984–2995. [PubMed: 22139901]
18. Zielonka J, Sikora A, Joseph J, Kalyanaraman B. Peroxynitrite is the major species formed from different flux ratios of co-generated nitric oxide and superoxide: direct reaction with boronate-based fluorescent probe. J. Biol. Chem. 2010; 285:14210–14216. [PubMed: 20194496]
19. Kumar A, Ganini D, Deterding LJ, Ehrenshaft M, Chatterjee S, Mason RP. Immuno-spin trapping of heme-induced protein radicals: Implications for heme oxygenase-1 induction and heme degradation. Free Radic. Biol. Med. 2013; 61C:265–272. [PubMed: 23624303]
20. Wang MJ, Lin WW, Chen HL, Chang YH, Ou HC, Kuo JS, Hong JS, Jeng KC. Silymarin protects dopaminergic neurons against lipopolysaccharide-induced neurotoxicity by inhibiting microglia activation. Eur. J. Neurosci. 2002; 16:2103–2112. [PubMed: 12473078]
21. Miller EW, Albers AE, Pralle A, Isacoff EY, Chang CJ. Boronate-based fluorescent probes for imaging cellular hydrogen peroxide. J. Am. Chem. Soc. 2005; 127:16652–16659. [PubMed: 16305254]
22. Davies MJ. The oxidative environment and protein damage. Biochim. Biophys. Acta. 2005; 1703:93–109. [PubMed: 15680218]
23. Winterbourn CC. Reconciling the chemistry and biology of reactive oxygen species. Nat. Chem. Biol. 2008; 4:278–286. [PubMed: 18421291]

24. Davies MJ, Gilbert BC, Haywood RM. Radical-induced damage to proteins: e.s.r. spin-trapping studies. Free Radic. Res. Commun. 1991; 15:111–127. [PubMed: 1661698]
25. Lashuel HA, Overk CR, Oueslati A, Masliah E. The many faces of alpha-synuclein: from structure and toxicity to therapeutic target. Nat. Rev. Neurosci. 2013; 14:38–48. [PubMed: 23254192]
26. Oueslati A, Schneider BL, Aebischer P, Lashuel HA. Polo-like kinase 2 regulates selective autophagic alpha-synuclein clearance and suppresses its toxicity in vivo. Proc. Natl. Acad. Sci. U.S.A. 2013; 110(41):E3945–E3954. [PubMed: 23983262]
27. Fu RH, Wang YC, Chen CS, Tsai RT, Liu SP, Chang WL, Lin HL, Lu CH, Wei JR, Wang ZW, Shyu WC, Lin SZ. Acetylcorynoline attenuates dopaminergic neuron degeneration and alpha-synuclein aggregation in animal models of Parkinson's disease. Neuropharmacology. 2013 In Press.
28. Zhai Z, Gomez-Mejiba SE, Gimenez MS, Deterding LJ, Tomer KB, Mason RP, Ashby MT, Ramirez DC. Free radical-operated proteotoxic stress in macrophages primed with lipopolysaccharide. Free Radic. Biol. Med. 2012; 53:172–181. [PubMed: 22580125]
29. Song JD, Lee SK, Kim KM, Kim JW, Kim JM, Yoo YH, Park YC. Redox factor-1 mediates NF-kappaB nuclear translocation for LPS-induced iNOS expression in murine macrophage cell line RAW 264.7. Immunology. 2008; 124:58–67. [PubMed: 18028373]
30. Lambeth JD. NOX enzymes and the biology of reactive oxygen. Nat. Rev. Immunol. 2004; 4:181–189. [PubMed: 15039755]
31. Clement HW, Vazquez JF, Sommer O, Heiser P, Morawietz H, Hopt U, Schulz E, von Dobschutz E. Lipopolysaccharide-induced radical formation in the striatum is abolished in Nox2 gp91phox-deficient mice. J. Neural Transm. 2010; 117:13–22. [PubMed: 19866338]
32. Cadenas E, Davies KJ. Mitochondrial free radical generation, oxidative stress, and aging. Free Radic. Biol. Med. 2000; 29:222–230. [PubMed: 11035250]
33. Xia Y, Zweier JL. Superoxide and peroxynitrite generation from inducible nitric oxide synthase in macrophages. Proc. Natl. Acad. Sci. U.S.A. 1997; 94:6954–6958. [PubMed: 9192673]
34. Gorlach A, Klappa P, Kietzmann T. The endoplasmic reticulum: folding, calcium homeostasis, signaling, and redox control. Antioxid. Redox Signal. 2006; 8:1391–1418. [PubMed: 16986999]
35. Bhattacharjee S, Deterding LJ, Jiang J, Bonini MG, Tomer KB, Ramirez DC, Mason RP. Electron transfer between a tyrosyl radical and a cysteine residue in hemoproteins: spin trapping analysis. J. Am. Chem. Soc. 2007; 129:13493–13501. [PubMed: 17939657]
36. Nakai K, Mason RP. Immunochemical detection of nitric oxide and nitrogen dioxide trapping of the tyrosyl radical and the resulting nitrotyrosine in sperm whale myoglobin. Free Radic. Biol. Med. 2005; 39:1050–1058. [PubMed: 16198232]
37. Chen YR, Chen CL, Liu X, Li H, Zweier JL, Mason RP. Involvement of protein radical, protein aggregation, and effects on NO metabolism in the hypochlorite-mediated oxidation of mitochondrial cytochrome c. Free Radic. Biol. Med. 2004; 37:1591–1603. [PubMed: 15477010]
38. Gunther MR, Sturgeon BE, Mason RP. Nitric oxide trapping of the tyrosyl radicalchemistry and biochemistry. Toxicology. 2002; 177:1–9. [PubMed: 12126791]
39. Shimohama S, Tanino H, Kawakami N, Okamura N, Kodama H, Yamaguchi T, Hayakawa T, Nunomura A, Chiba S, Perry G, Smith MA, Fujimoto S. Activation of NADPH oxidase in Alzheimer's disease brains. Biochem. Biophys. Res. Commun. 2000; 273:5–9. [PubMed: 10873554]
40. Hensley K, Maidt ML, Yu Z, Sang H, Markesbery WR, Floyd RA. Electrochemical analysis of protein nitrotyrosine and dityrosine in the Alzheimer brain indicates region-specific accumulation. J. Neurosci. 1998; 18:8126–8132. [PubMed: 9763459]
41. Palazzolo-Ballance AM, Suquet C, Hurst JK. Pathways for intracellular generation of oxidants and tyrosine nitration by a macrophage cell line. Biochemistry. 2007; 46:7536–7548. [PubMed: 17530864]
42. Pfeiffer S, Lass A, Schmidt K, Mayer B. Protein tyrosine nitration in cytokine-activated murine macrophages. Involvement of a peroxidase/nitrite pathway rather than peroxynitrite. J. Biol. Chem. 2001; 276:34051–34058. [PubMed: 11425852]
43. Blasi E, Barluzzi R, Bocchini V, Mazzolla R, Bistoni F. Immortalization of murine microglial cells by a v-raf/v-myc carrying retrovirus. J. Neuroimmunol. 1990; 27:229–237. [PubMed: 2110186]

44. Giulian D, Baker TJ. Characterization of ameboid microglia isolated from developing mammalian brain. J. Neurosci. 1986; 6:2163–2178. [PubMed: 3018187]
45. Ischiropoulos H, Zhu L, Beckman JS. Peroxynitrite formation from macrophage-derived nitric oxide. Arch. Biochem. Biophys. 1992; 298:446–451. [PubMed: 1329657]
46. He YF, Chen HJ, Qian LH, He LF, Buzby JS. Diphenyleneiodonium protects preoligodendrocytes against endotoxin-activated microglial NADPH oxidase-generated peroxynitrite in a neonatal rat model of periventricular leukomalacia. Brain Res. 2013; 1492:108–121. [PubMed: 23174417]
47. Sikora A, Zielonka J, Lopez M, Joseph J, Kalyanaraman B. Direct oxidation of boronates by peroxynitrite: mechanism and implications in fluorescence imaging of peroxynitrite. Free Radic. Biol. Med. 2009; 47:1401–1407. [PubMed: 19686842]
48. Han W, Li H, Cai J, Gleaves LA, Polosukhin VV, Segal BH, Yull FE, Blackwell TS. NADPH oxidase limits lipopolysaccharide-induced lung inflammation and injury in mice through reduction-oxidation regulation of NF-kappaB activity. J. Immunol. 2013; 190:4786–4794. [PubMed: 23530143]
49. Conti A, Miscusi M, Cardali S, Germano A, Suzuki H, Cuzzocrea S, Tomasello F. Nitric oxide in the injured spinal cord: synthases cross-talk, oxidative stress and inflammation. Brain Res. Rev. 2007; 54:205–218. [PubMed: 17500094]
50. Hague S, Peuralinna T, Eerola J, Hellstrom O, Tienari PJ, Singleton AB. Confirmation of the protective effect of iNOS in an independent cohort of Parkinson disease. Neurology. 2004; 62:635–636. [PubMed: 14981185]

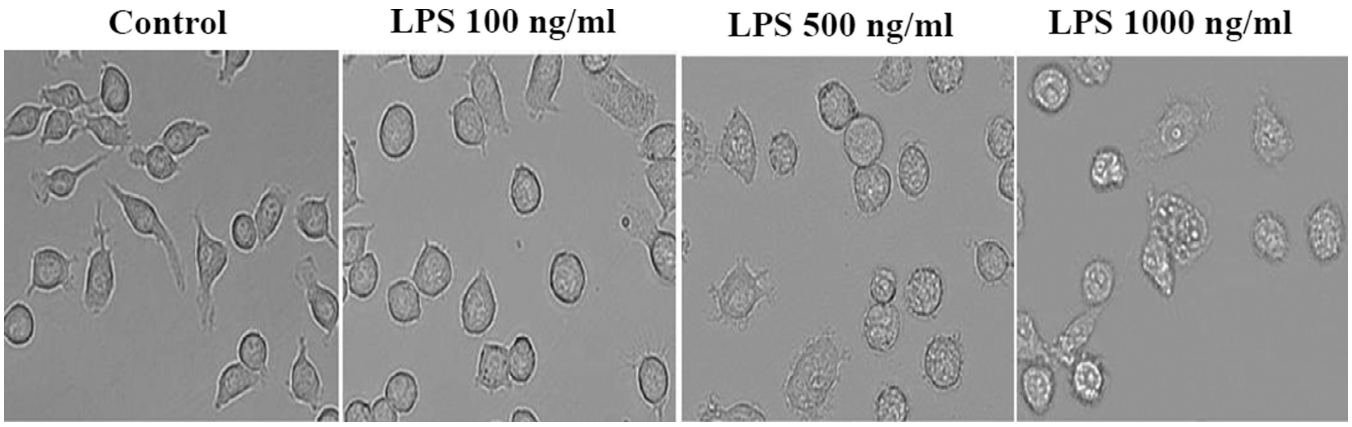

Figure 1.

LPS triggers microglial activation and changes in morphology. Phase contrast images showing morphology of BV2 cells treated with different concentrations of LPS for 24 hours.

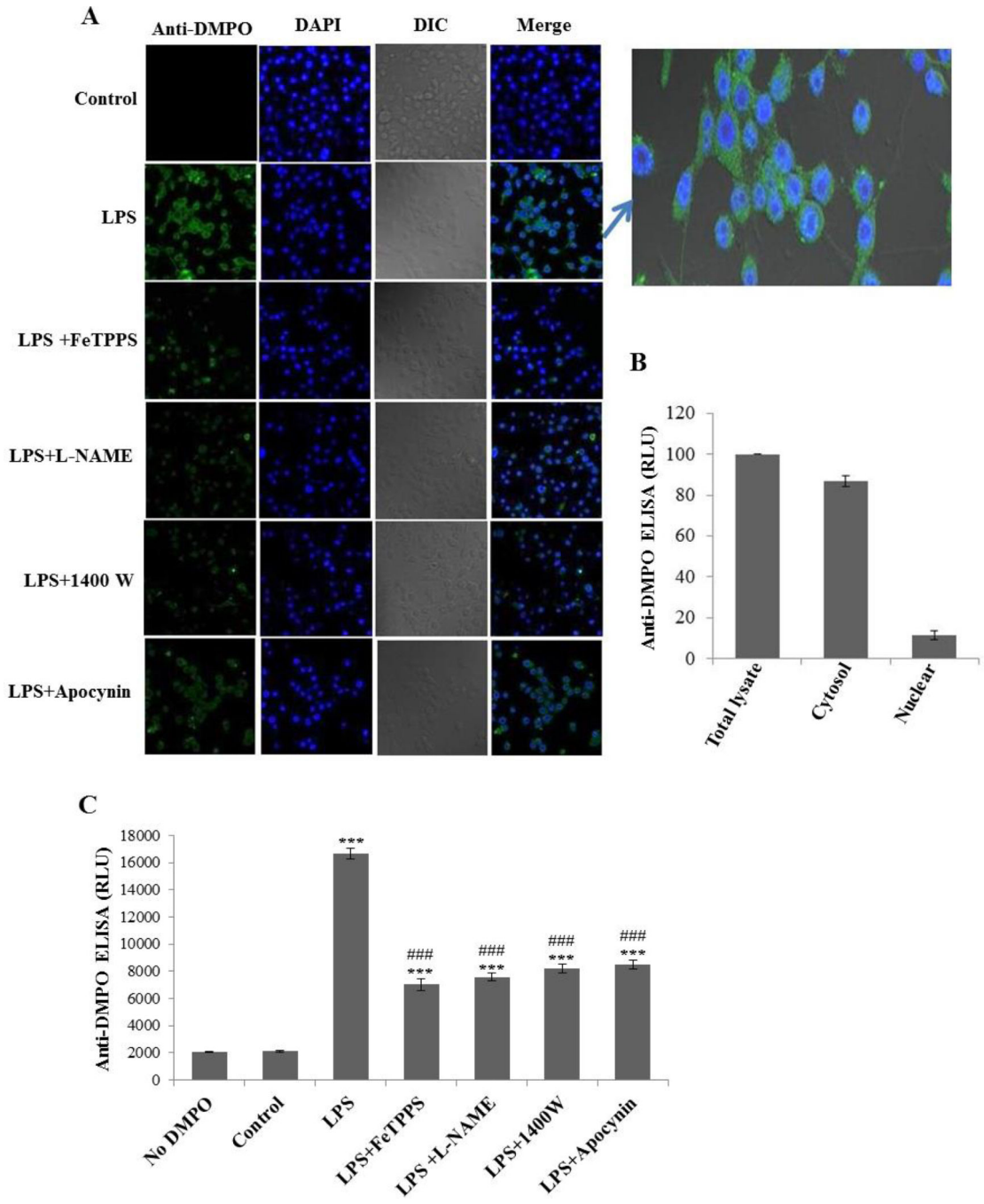

Figure 2.

LPS induces protein radical formation in BV2 cells. (A) Confocal images showing the anti-DMPO staining of BV2 cells treated with 500 ng/ml LPS and 50 mM DMPO for 24 hours in the presence and absence of pretreatment with FeTPPS (10 μM), L-NAME (100 μM), 1400W (10 μM), and apocynin (1 mM). (B) Anti-DMPO ELISA from the nuclear and cytosolic fractions of LPS-treated BV2 cells. (C) Anti-DMPO ELISA of BV2 cells treated with 500 ng/ml LPS and 50 mM DMPO for 24 hours in the presence and absence of pretreatment with FeTPPS (10 μM), L-NAME (100 μM), 1400W (10 μM), and apocynin (1

mM). Data show mean values ± SEM or representative images from three independent experiments (n=6). (*** P<0.001, with respect to control, and ### P<0.001, with respect to the LPS-treated group.)

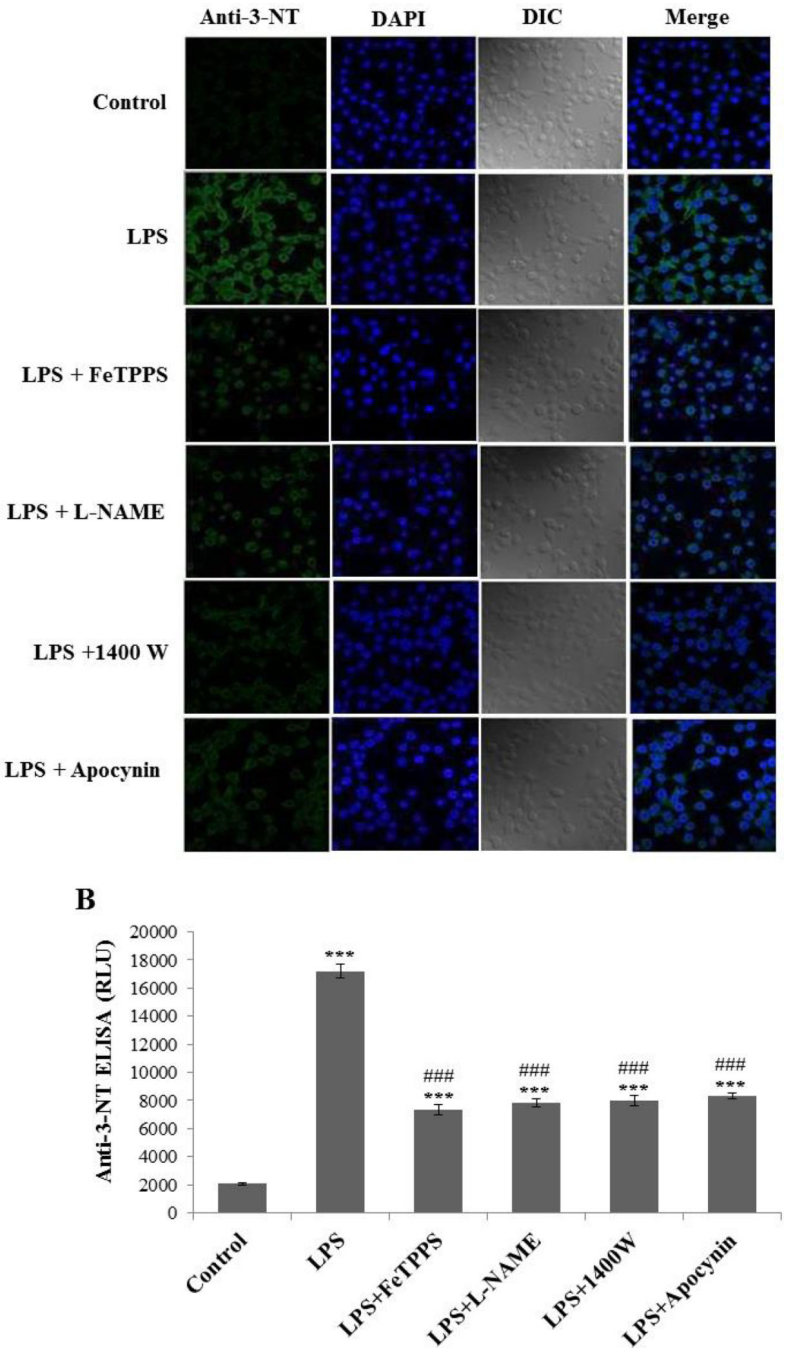

Figure 3.

LPS induces tyrosine nitration in BV2 cells. (A) Confocal images showing anti-3-nitro-tyrosine staining of BV2 cells treated with 500 ng/ml LPS and 50 mM DMPO for 24 hours in the presence and absence of pretreatment with FeTPPS (10 μM), L-NAME (100 μM), 1400W (10 μM), and apocynin (1 mM). (B) Anti-nitrotyrosine ELISA of BV2 cells treated with 500 ng/ml LPS and 50 mM DMPO for 24 hours in the presence and absence of pretreatment with FeTPPS (10 μM), L-NAME (100 μM), 1400W (10 μM), and apocynin (1 mM). Data show mean values ± SEM or representative images from three independent

experiments (n=6). (*** P<0.001, with respect to control, and ### P<0.001, with respect to the LPS-treated group.)

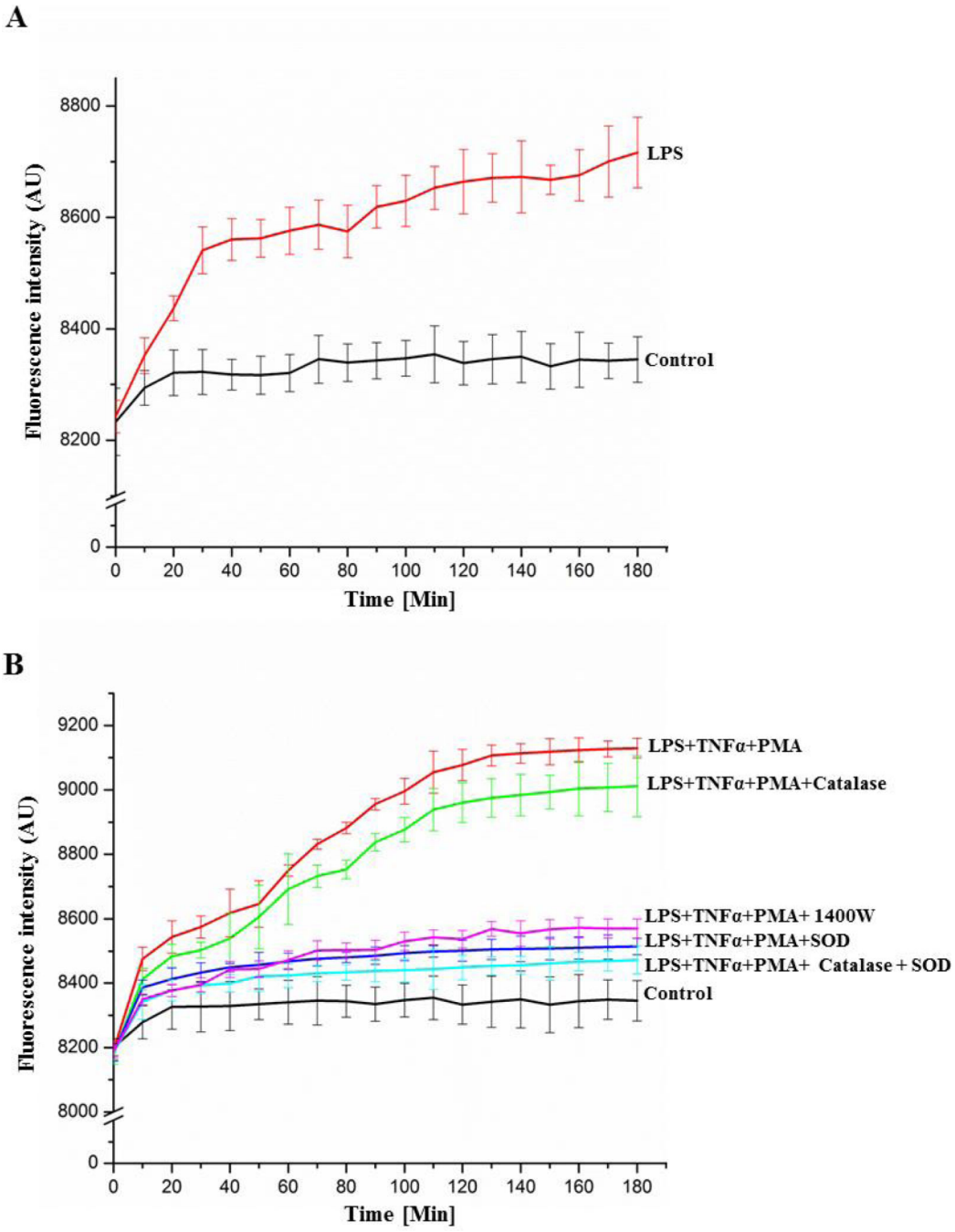

Figure 4.

Measurement of peroxynitrite formation by monitoring the oxidation of coumarin-7-boronic acid. (A) Cells were incubated with LPS (500 ng/ml) for 21 hours and then CBA was added (20 μM) to the medium. (B) Cells were incubated with LPS (500 ng/ml) and TNFα (50 ng/ml) in the presence and absence of the iNOS inhibitor 1400W (10 μM) for 21 hours, and then co-treated with CBA and PMA (200 ng/ml) in the same medium. Additionally, in some samples, the $O_2^{\bullet-}$ scavenger SOD (500 U/ml) and/or the H_2O_2 scavenger catalase (1000

U/ml) were added along with CBA and PMA. Continuous fluorescence intensity measurements were initiated immediately after CBA was added.

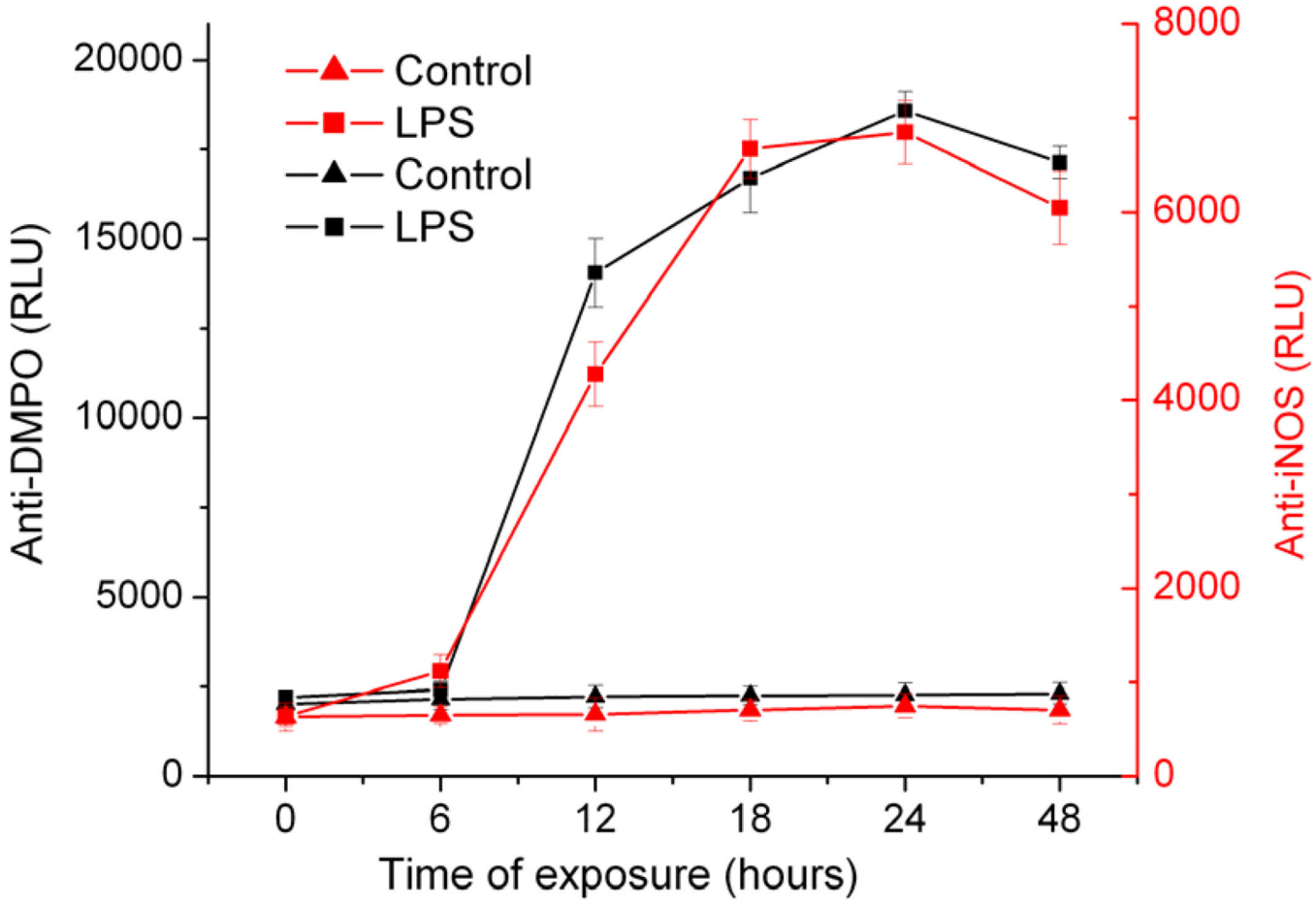

Figure 5.

Correlation between iNOS expression and protein radical formation. Anti-DMPO and anti-iNOS ELISA of BV2 cells exposed to 500 ng/ml LPS and 50 mM DMPO (0–48 hours). Data show mean values ± SEM from three independent experiments (n=6).

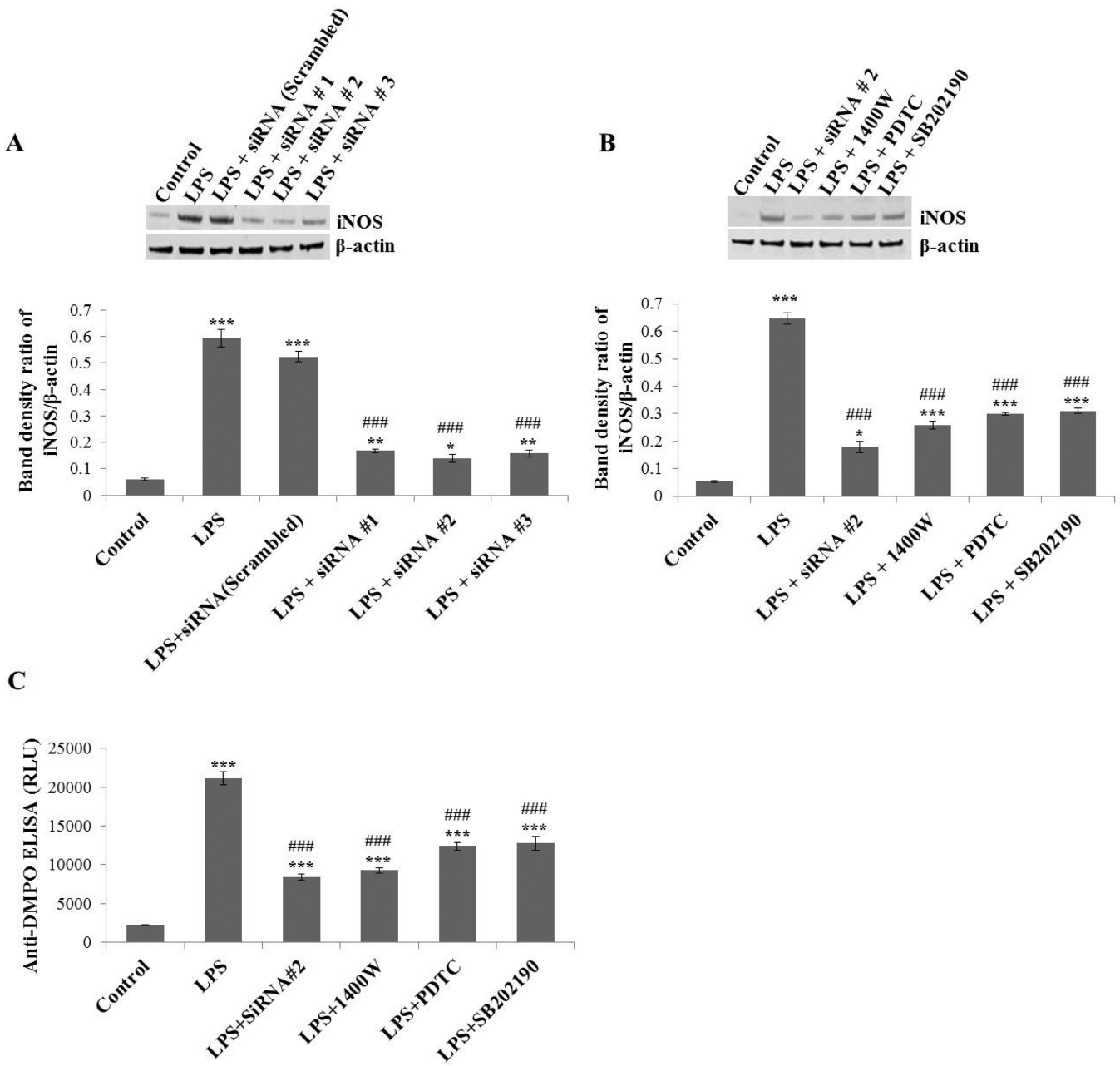

Figure 6.

Effect of iNOS inhibition/silencing on LPS-induced protein oxidation in BV2 cells. (A) BV2 cells were transfected with siRNA1, 2, 3 of iNOS or control (scrambled) siRNA. Forty-eight hours later, cells were incubated with LPS (500 ng/ml) for 24 hours and then harvested for Western blot. The upper panel shows a Western blot of iNOS and the lower panel shows the band density ratio of iNOS and β-actin. (B) BV2 cells transfected with most effective siRNA#2 for iNOS or cells exposed to direct (1400W) or indirect (PDTC, SB202190) inhibitors of iNOS were analyzed by Western blot (upper panel). The lower panel shows the band density ratio of iNOS and β-actin. (C) Anti-DMPO ELISA of BV2 cells treated with 500 ng/ml LPS and 50 mM DMPO for 24 hours in the presence and absence of iNOS

silencing/inhibition. Data show mean values ± SEM or representative images from three independent experiments (n=6). (*P<0.05, ** P<0.01, *** P<0.001, with respect to control, and ### P<0.001, with respect to the LPS-treated group.

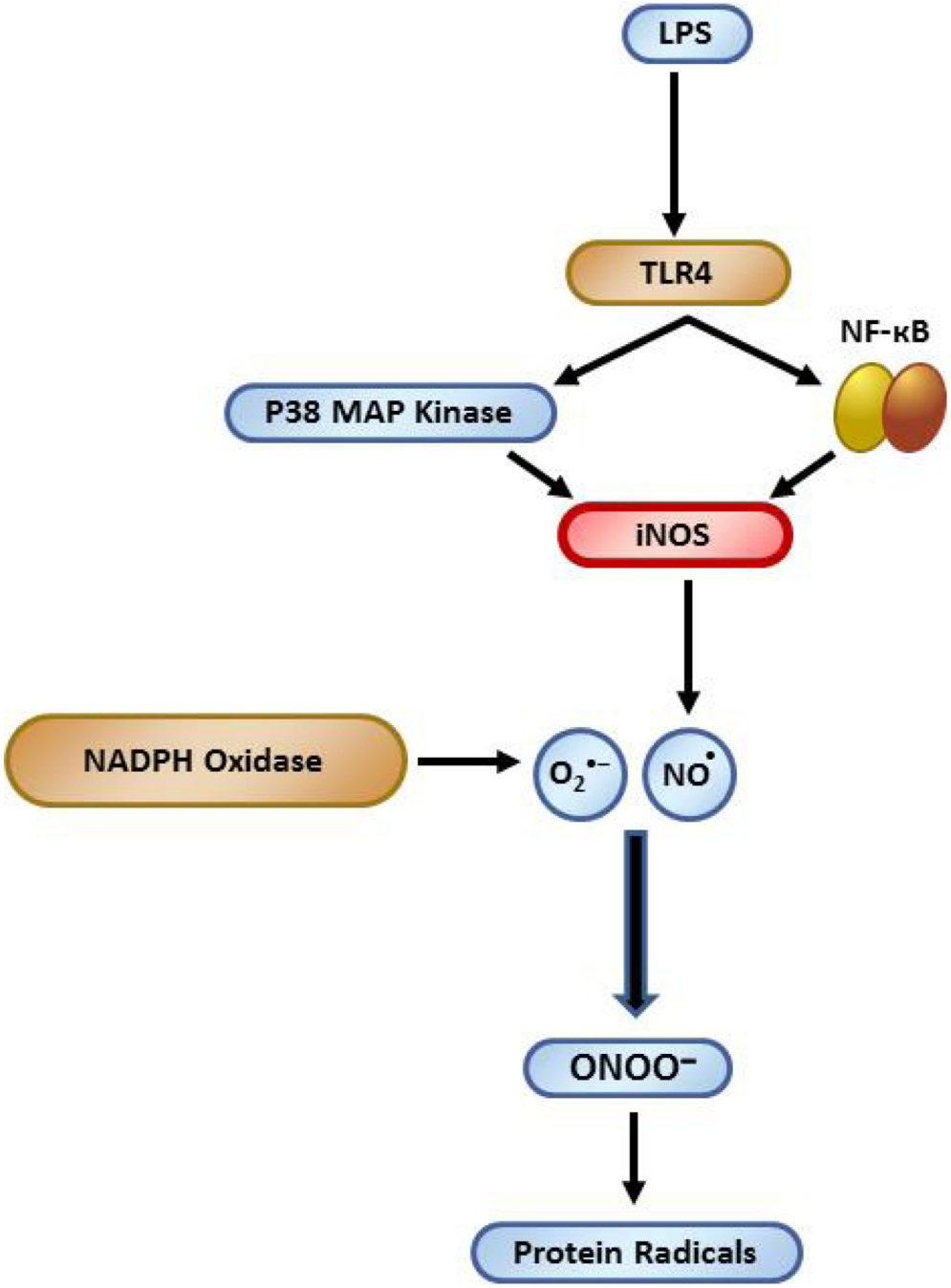

Scheme.

iNOS is crucial to LPS-induced protein radical formation in microglia

Role of iNOS in LPS-induced protein radical formation in BV2 cells.